Discrete Mathematics Letters
www.dmlett.com

Discrete Math. Lett. **9** (2022) 111–117
DOI: 10.47443/dml.2021.s218

Research Article

A curious family of convex benzenoids and their altans

Nino Bašić[1,2,3], Patrick W. Fowler[4,*]

[1]*FAMNIT (Faculty of Mathematics, Natural Sciences and Information Technologies), University of Primorska, Koper, Slovenia*
[2]*IAM (Inštitut Andrej Marušič), University of Primorska, Koper, Slovenia*
[3]*Institute of Mathematics, Physics and Mechanics, Ljubljana, Slovenia*
[4]*Department of Chemistry, University of Sheffield, Sheffield, UK*

(Received: 30 April 2022. Received in revised form: 5 May 2022. Accepted: 16 May 2022. Published online: 19 May 2022.)

Abstract

The altan graph of G, $\mathfrak{a}(G,H)$, is constructed from graph G by choosing an *attachment set* H from the vertices of G and attaching vertices of H to alternate vertices of a new perimeter cycle of length $2|H|$. When G is a polycyclic plane graph with maximum degree 3, the *natural choice* for the attachment set is to take all perimeter degree-2 vertices in the order encountered in a walk around the perimeter. The construction has implications for the electronic structure and chemistry of carbon nanostructures with molecular graph $\mathfrak{a}(G,H)$, as kernel eigenvectors of the altan correspond to non-bonding π molecular orbitals of the corresponding unsaturated hydrocarbon. Benzenoids form an important subclass of carbon nanostructures. A *convex benzenoid* has a boundary on which all vertices of degree 3 have exactly two neighbours of degree 2. The *nullity* of a graph is the dimension of the kernel of its adjacency matrix. The possible values for the excess nullity of $\mathfrak{a}(G,H)$ over that of G are 2, 1, or 0. Moreover, altans of benzenoids have nullity at least 1. Examples of benzenoids where the excess nullity is 2 were found recently. It has been conjectured that the excess nullity when G is a convex benzenoid is at most 1. Here, we exhibit an infinite family of convex benzenoids with 3-fold dihedral symmetry (point group $\mathbf{D}_{3\mathrm{h}}$) where nullity increases from 2 to 3 under altanisation. This family accounts for all known examples with the excess nullity of 1 where the parent graph is a singular convex benzenoid.

Keywords: altan; nullity; chemical graph; benzenoid; convex benzenoid; point-group symmetry.

2020 Mathematics Subject Classification: 05C92, 05C50, 15A18.

1. Introduction

This short paper is dedicated to the memory of Nenad Trinajstić, a pioneer of Chemical Graph Theory, the interdiscipline that he named [31–33], which builds on the legacy of theoretical chemists such as Hückel, Coulson, McWeeny, and Longuet-Higgins [7–11, 24, 27] who constructed fruitful qualitative mathematical explanations for chemical trends. The focus of the present paper is an aspect of the theory of non-bonding π orbitals. In Hückel Theory of π systems [7–11], a non-bonding π orbital corresponds to an eigenvector of the adjacency matrix of the graph of a conjugated carbon framework (which may be part of a fragment of graphene, a polycyclic aromatic hydrocarbon, or an extended nanostructure) that has eigenvalue zero (i.e. belongs to the kernel of the adjacency matrix). Non-bonding orbitals are important in chemistry, as they signal the ability of a π system to undergo facile loss or gain of electrons, and they are implicated in theories of molecular conduction [17]. Pencil-and-paper methods for establishing the count of non-bonding π molecular orbitals (the size of the kernel, i.e. the *nullity* of the molecular graph) have a long history [14,26,33,36]. Mathematical theory of nullity in graph spectra has been reviewed in [21].

One recent development in Chemical Graph Theory in which nullity plays a significant part is in the theory of altans [1,2,4,15,19,20,28,35]. These are conjugated π systems formally derived from the molecular graph of a conjugated parent π system by circumscribing it with a large cycle. In chemical terms, we take an annulene and attach it via alternate degree-2 vertices to the parent. The resulting structure is known as an *altan*. Figure 1 shows an example of this construction, which can also be seen as replacement of perimeter CH bonds of a planar patch with vinyl groups that then cyclise [19]. In this context, a *patch* is a sub-cubic 2-connected plane graph that has each degree-2 vertex incident with the distinguished outer face. The structure of the altan depends on both the parent graph G and the set of attachment vertices H, and hence the altan is denoted $\mathfrak{a}(G,H)$; see [1] for further details. When H is the natural attachment set, we can abbreviate the notation to $\mathfrak{a}(G)$. In the standard procedure from the chemical literature, the natural attachment set for a patch is an h-tuple that contains all degree-2 vertices of the patch in the order induced by clockwise traversal of the perimeter (i.e. the outer face).

*Corresponding author (p.w.fowler@sheffield.ac.uk).

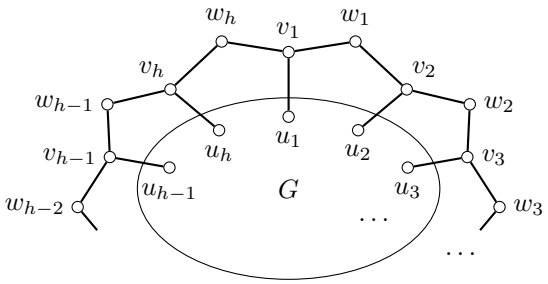

Figure 1: The altan $\mathfrak{a}(G,H)$. Attachment of the annulene to the graph G is via the set $H=\{u_1,\ldots,u_h\}$ of vertices in G to alternate vertices of the annulene $\{v_1,v_2,\ldots,v_h\}$, and the perimeter of the altan $\mathfrak{a}(G,H)$ is the cycle $\{v_1,w_1,\ldots,v_h,w_h\}$.

The 'altanisation' process gives a formal device for understanding tubular nanostructures with hydrocarbon patches as caps. Observations published in the chemical literature, where the construction originated, have been formalised in the mathematical chemistry literature [1, 19, 20]: it is known that nullity of an altan can exceed that of the parent graph by $0, 1$ or 2 (only), and all three cases occur for benzenoids [1]. (A *fusene* is a simple planar 2-connected graph embedded in the plane such that all internal faces are hexagons, all vertices not on the external face have degree 3 and vertices on the external face have degree 2 or 3 [6]. A *benzenoid* is a fusene that can be embedded in the infinite hexagonal lattice.) An early enumeration and visualisation of small benzenoids is given in books co-authored by Nenad Trinajstić [25, 34].

An intriguing observation made recently in [1] is that, for *convex benzenoids* [3, 13], it appears that the excess nullity of the altan over the parent is at most 1. In particular, extensive computations suggest that the excess for Kekulean (equivalently, non-singular) convex benzenoids is always 1, and that for non-Kekulean (equivalently, singular) benzenoids the excess is always either 0 or 1. The present note deals with this second case, and provides a mathematical framework for understanding an infinite family of singular benzenoids for which the excess nullity is 1.

In the classification described in [3], the members of this family have a truncated triangular shape with a fixed difference of 2 in the two distinct side lengths, i.e. they belong to the class of *hexagonal benzenoids* $H(n,m,k,t)$, having n hexagons on the base, m hexagons on the left side, k hexagons on the right side and t hexagons on the top side. More precisely, they belong to the subclass $H(k+2,k,k,k)$, where $k\geq 1$ ($k=1$ is the degenerate case of the equilateral triangle $T_3(3)$ in the notation used in [3]). The corresponding boundary-edges code [23] is $32^k32^{k-2}32^k32^{k-2}32^k32^{k-2}$.

It turns out that this family accounts for all those cases of convex benzenoids with nullity 2 and altan nullity 3 found in the computer search of the $760\,511$ convex benzenoids on up to $3\,000$ faces reported in [1]. We conjecture that this family gives *all* cases where a singular convex benzenoid has excess nullity 1 on altanisation. Whether or not this is true, the computer search already assures us that no counterexamples to the conjecture are accessible by conventional small-molecule synthetic methods. Nullity properties of this special family of convex benzenoids and altans are proved here.

2. The family of truncated triangular convex benzenoids

The general member of the family is shown in Figure 2, along with the three smallest examples. We start from the experimentally accessible [30] second member of the triangulene family, which is the case with $k=1$, and increase both long and short sides by one hexagon at each step. Note that the benzenoid $H(k+2,k,k,k)$ has $3k(k+1)$ hexagonal faces and $6k^2+12k+4$ vertices, which are partitioned into $3k^2+6k+3$ black (starred) and $3k^2+6k+1$ white (unstarred) vertices. The natural attachment set has size $6k+6$. It is easy to show the following proposition about nullity of members of this family:

Proposition 2.1. *$\eta(H(k+2,k,k,k))=2$ for all $k\geq 1$.*

Proof. Let $\pi(B),\nu(B)$ and $\eta(B)$ denote the numbers of positive, negative and zero eigenvalues of B, respectively, and let $\beta(B)$ denote the matching number (also known as edge independence number) of B. By [16, Theorem 1], $\pi(B)=\nu(B)=\beta(B)$. Hence, $\eta(B)=n(B)-2\beta(B)$, where $n(B)$ denotes the number of vertices of B. The colour excess of 2 gives a bound on β, namely $\beta(B)\leq n(B)-2/2$. Explicit construction shows that equality applies for the benzenoids in this family. Connect the k peaks to k arbitrarily chosen valleys (one to peak to one valley) using disjoint monotonic paths [22], leaving out two valleys. Now construct the matching using all non-vertical edges on the paths and all vertical edges in the remainder of the graph. This yields a maximum matching covering all vertices apart from the two leftover valleys, hence $\eta(B)=2$. □

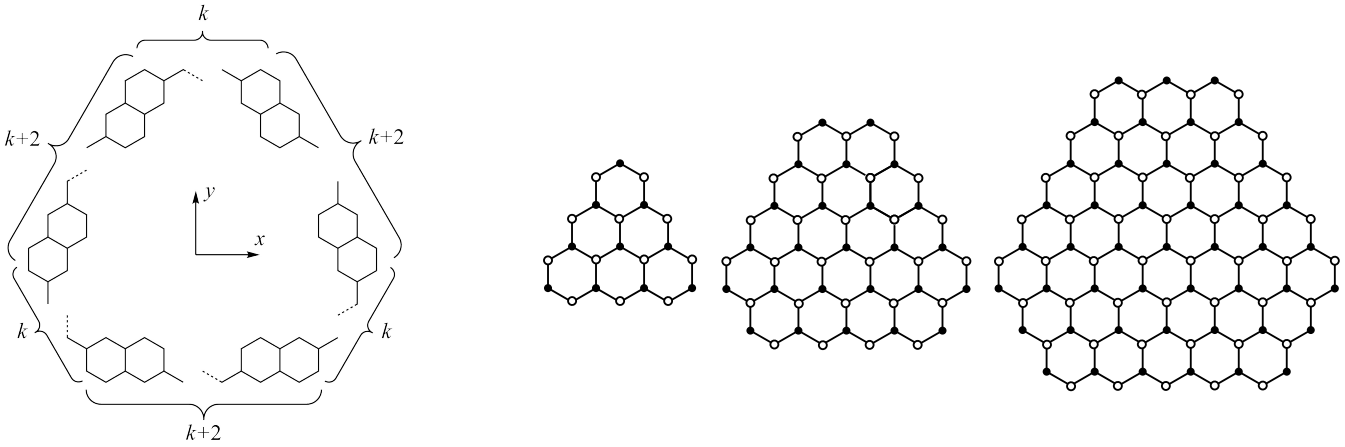

(a) (b)

Figure 2: A family of convex benzenoids. (a) Schematic construction of the benzenoid $H(k+2,k,k,k)$. (b) The three smallest members of the family: $H(3,1,1,1) \cong T_3(3)$, $H(4,2,2,2)$, and $H(5,3,3,3)$. Coordinates (x,y) are defined relative to the central atom in an embedding that has regular hexagonal faces with two vertical edges and unit edge-length.

We can extend Proposition 2.1 using arguments from point-group theory. For our purpose, it is sufficient to describe the family $H(k+2,k,k,k)$ using the $\mathbf{D}_3$ point group. In a chemical context, $\mathbf{D}_{3h}$ is the maximum point group of the planar benzenoid in 3D space equipped with p_π orbitals (antisymmetric with respect to the molecular plane); $\mathbf{D}_3$ would be the group in a 'pseudo-π' model [18], where we ignore the third dimension and model π systems with σ orbitals. We can always reconstitute the full π symmetry: simply multiply the σ representation (permutation representation of the vertices of B), $\Gamma(V(B),k)$ by the representation of an out-of-plane vector (see [18] for details). Calculation of characters for the general member of the $H(k+2,k,k,k)$ family gives

$\mathbf{D}_3$	E	$2C_3$	$3C_2'$
$\Gamma(V(B),k)$	$6k^2+12k+4$	1	$2k+2$

where the entry for each class of operations (E = identity; C_3 = rotation by $\frac{2\pi}{3}$ about a normal to the plane; C_2' = rotation by π about an in-plane 2-fold axis or equivalently reflection in an in-plane mirror line) is the number of vertices unshifted by each operation in that class. The standard reduction technique [5] gives the reducible representation:

$$\Gamma(V(B),k) = (k^2+3k+2)A_1 + (k^2+k)A_2 + (2k^2+4k+1)E, \tag{1}$$

where A_1 and A_2 are non-degenerate, and E is the 2-fold degenerate irreducible representation of $\mathbf{D}_3$. Now we use the Coulson-Rushbrooke Pairing Theorem [12], which asserts that if λ is a non-zero eigenvalue of the adjacency matrix of a bipartite graph, then $-\lambda$ is also an eigenvalue, and furthermore that from an eigenvector for λ it is possible to construct an eigenvector for $-\lambda$ by reversing the entries on one partite set. In symmetry terms, this leads to the relationship between the reducible representations of bonding and anti-bonding ($\lambda > 0$ vs $\lambda < 0$) eigenspaces (shells of molecular orbitals)

$$\Gamma(\lambda > 0) = \Gamma_* \times \Gamma(\lambda < 0), \tag{2}$$

and a nonbonding ($\lambda = 0$) space that is self-paired

$$\Gamma(\lambda = 0) = \Gamma_* \times \Gamma(\lambda = 0), \tag{3}$$

where Γ_* is the irreducible representation of a vector with entries $+1$ on black, and -1 on white vertices of B. In the case of the family $H(k+2,k,k,k)$, Γ_* is the totally symmetric representation, i.e. A_1 in $\mathbf{D}_3$. As k^2+3k+2 and k^2+k are even and $2k^2+4k+1$ is odd, it follows that the representation for the kernel eigenspace must be the doubly degenerate representation E for all members of this family.

Furthermore, we can span the kernel, $\ker B$, with two independent vectors, one of which, denoted by $\mathbf{x}$, is antisymmetric with respect to reflection in the y axis (see Figure 2), and the other of which is obtained by rotation of $\mathbf{x}$ by $\frac{2\pi}{3}$. Independence is clear, as the antisymmetric vector $\mathbf{x}$ is also part of an orthogonal pair $(\mathbf{x},\mathbf{y})$ spanning E (see Figure 3), which transform under the operation C_3 into the pair $(-\frac{1}{2}\mathbf{x} - \frac{\sqrt{3}}{2}\mathbf{y}, \frac{\sqrt{3}}{2}\mathbf{x} - \frac{1}{2}\mathbf{y})$, and hence the rotated vector $C_3\mathbf{x}$ is not collinear to $\mathbf{x}$.

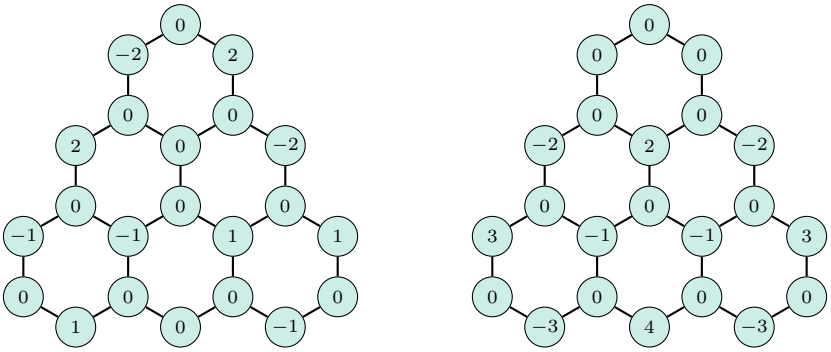

(a) $k = 1$

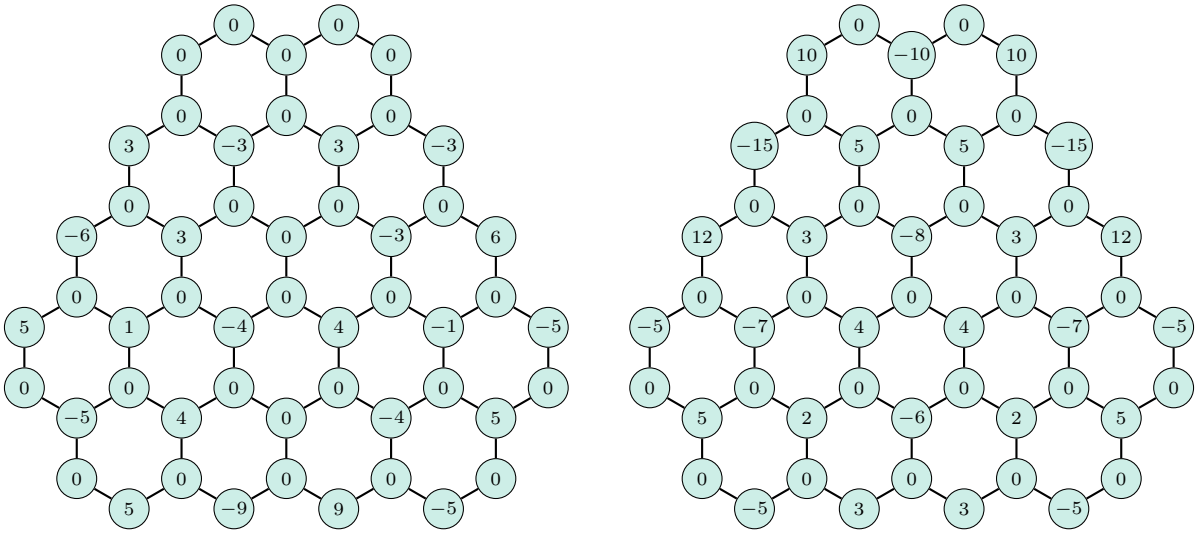

(b) $k = 2$

Figure 3: The orthogonal pair $(\mathbf{x}, \mathbf{y})$ transforming as the E irreducible representation of $\mathbf{D}_3$ for the two smallest members of the family $H(k+2, k, k, k)$. Unnormalised forms are shown, to give integer entries.

The significance of this particular choice of vectors will be made clear by considering the concept of *extendable* kernel eigenvectors, as defined in [1]. The essential results is as follows: Let $(G', H') = \mathfrak{a}(G, H)$ and let the vertices of G' be labelled as in Figure 1. For a kernel eigenvector $\mathbf{q}$ of $A(G)$ define the weighted sum of entries

$$\mathcal{C}(\mathbf{q}) = \sum_{i=1}^{h} (-1)^i \mathbf{q}(u_i). \tag{4}$$

If $\mathcal{C}(\mathbf{q}) = 0$ then the vector $\mathbf{q} \in \ker A(G)$ can be extended to a vector on the altan $\widetilde{\mathbf{q}} \in \ker A(G')$.

In our case, one kernel eigenvector is $\mathbf{x}$, built by attaching entry 0 to the central vertex of $H(k+2, k, k, k)$ and entries $0, +1$, and -1 to its neighbours in clockwise order, then systematically applying the local condition for a kernel vector:

$$\sum_{s \sim r} \mathbf{x}(s) = 0 \qquad \text{for all } r \in V(B). \tag{5}$$

The second kernel eigenvector is the rotation $C_3\mathbf{x}$, which is antisymmetric with respect to a rotated mirror plane, and hence $\mathcal{C}(\mathbf{x}) = \mathcal{C}(C_3\mathbf{x}) = 0$, and both vectors are extendable, as is any linear combination of them (see Figure 4(a)). A further kernel eigenvector is immediately available. This is $\mathbf{s}$, known as the special one [1], which has alternating $+1$ and -1 entries on vertices $w_1, w_2, \ldots, w_h$ and 0 on all other vertices of $\mathfrak{a}(B)$. This is formally an extension of the all-zero vector on the vertices of B. The vector $\mathbf{s}$ has representation A_1 (resp. A_2) in members of the family with even (resp. odd) k. By symmetry, therefore, in both cases $\mathbf{s}$ is orthogonal to the E pair, and as $\mathbf{x}$ and $C_3\mathbf{x}$ are independent, $\ker \mathfrak{a}(B)$ has dimension ≥ 3. Taken together with [1, Theorem 5] on excess nullity of altans, we have the bounds

$$3 \leq \eta(\mathfrak{a}(B)) \leq 4, \tag{6}$$

for benzenoids in the $\{H(k+2, k, k, k) \mid k \geq 1\}$ family (with the natural choice of attachment set). To close the gap, it is useful to exploit the concept of *contractibility* [1] of kernel eigenvectors of the altan. Let $(G', H') = \mathfrak{a}(G, H)$ and let the vertices of G' be labelled as in Figure 1. A kernel eigenvector $\widetilde{\mathbf{q}} \in \ker A(G')$ is called *contractible* if $\widetilde{\mathbf{q}}(v_i) = 0$ for all $1 \leq i \leq h$. The contraction of $\widetilde{\mathbf{q}}$ is the vector $\mathbf{q}$ of G defined by $\mathbf{q}(u) = \widetilde{\mathbf{q}}(u)$ for $u \in V(G)$. An immediate consequence is that $\mathbf{q} \in \ker(G)$.

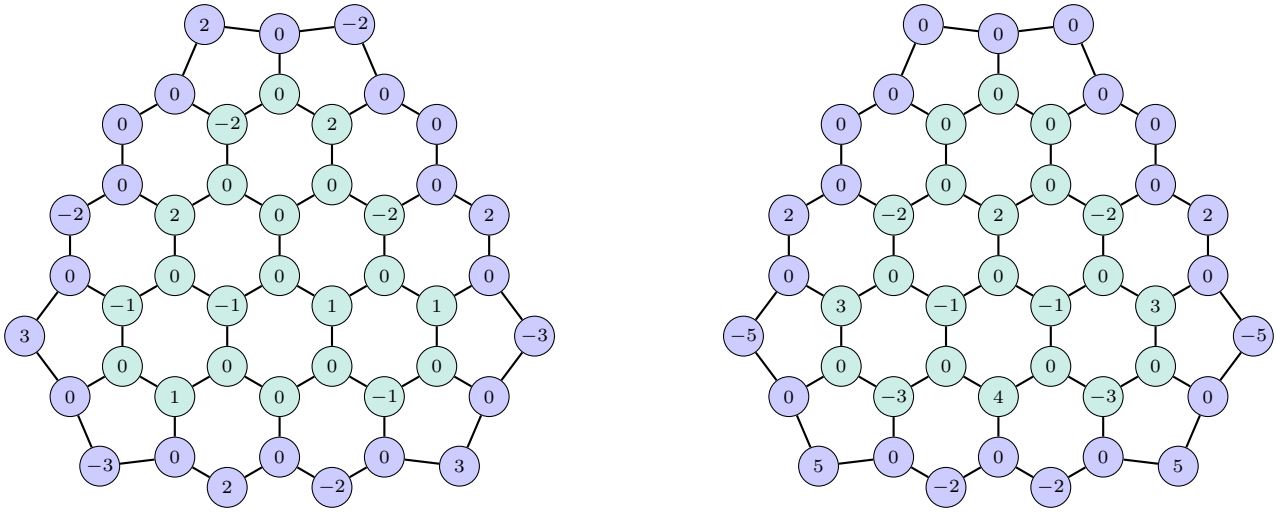

(a) (b)

Figure 4: Demonstration of extendability of an antisymmetric and a symmetric kernel eigenvector for $H(3,1,1,1)$. Arbitrary antisymmetric and symmetric extensions do not necessarily form a pure E pair.

Note that the extension of a kernel eigenvector always contracts back to itself. From [1, Proof of Theorem 5] it follows that if all vectors of $\ker \mathfrak{a}(B)$ are contractible then $\eta(\mathfrak{a}(B)) \leq \eta(B) + 1$. Hence, in cases where $\eta(\mathfrak{a}(B)) = \eta(B) + 2$, at least one vector from $\ker \mathfrak{a}(B)$ must be non-contractible.

We can use the reasoning that led to Equation (1) to determine the reducible representation of the full set of eigenvectors of the altan:

$\mathbf{D}_3$	E	$2C_3$	$3C_2'$
$\Gamma(V(\mathfrak{a}(B)),k)$	$6k^2+24k+16$	1	$2k+4$

and hence

$$\Gamma(V(\mathfrak{a}(B)),k) = (k^2+5k+5)A_1 + (k^2+3k+1)A_2 + (2k^2+8k+5)E. \tag{7}$$

The altan is non-bipartite, and so is not governed by the Coulson-Rushbrooke Pairing Theorem.

Recall that $\ker \mathfrak{a}(B)$ contains three independent vectors: $\mathbf{x}, C_3\mathbf{x}$, and $\mathbf{s}$. Suppose that it contained a fourth independent vector $\mathbf{m}$ (the '*magic*' vector). Note that $\mathbf{m}$ would have to be non-contractible, as $\eta(B) = 2$. We can place a symmetry limitation on this putative fourth vector. As the kernel already contains a vector of either A_1 or A_2 symmetry (namely, $\mathbf{s}$) and a pair of E symmetry, the extra vector $\mathbf{m}$ must belong to a non-degenerate irreducible representation of $\mathbf{D}_3$ (call it $\Gamma(\mathbf{m})$). Hence, we have four cases to test for contractibility, defined by whether $\Gamma(\mathbf{m})$ is A_1 or A_2 and by the parity of k.

Two cases are easily decided. First, if $\Gamma(\mathbf{m}) = A_2$ and k is odd, all perimeter degree-3 vertices of the altan carry a zero entry, propagated from a single zero on the C_2' axis on the perimeter, and hence the vector $\mathbf{m}$ is contractible, a contradiction. Secondly, if $\Gamma(\mathbf{m}) = A_1$ and k is even, there is a degree-2 vertex w on a C_2' axis, and the entries in $\mathbf{m}$ on its neighbours are equal (from A_1 symmetry) and opposite (from the local condition), so these entries vanish. As before, the zeros propagate and $\mathbf{m}$ is contractible, a contradiction. Our proofs for the remaining two cases are more technical, but both lead to the same conclusion: assumption of a non-contractible vector $\mathbf{m}$ leads to a contradiction. We show only the case for $\Gamma(\mathbf{m}) = A_2$ and even k in detail; the case for $\Gamma(\mathbf{m}) = A_1$ and odd k odd proceeds in a closely similar way, with allowance for the different boundary conditions. Two cases are easily decided. First, if $\Gamma(\mathbf{m}) = A_2$ and k is odd, all perimeter degree-3 vertices of the altan carry a zero entry, propagated from a single zero on the C_2' axis on the perimeter, and hence the vector $\mathbf{m}$ is contractible, a contradiction. Secondly, if $\Gamma(\mathbf{m}) = A_1$ and k is even, there is a degree-2 vertex w on a C_2' axis, and the entries in $\mathbf{m}$ on its neighbours are equal (from A_1 symmetry) and opposite (from the local condition), so these entries vanish. As before, the zeros propagate and $\mathbf{m}$ is contractible, a contradiction.

Our proofs for the remaining two cases are more technical, but both lead to the same conclusion: assumption of a non-contractible vector $\mathbf{m}$ leads to a contradiction. We sketch the proof only for the case $\Gamma(\mathbf{m}) = A_2$ and even k; the case for $\Gamma(\mathbf{m}) = A_1$ and odd k proceeds in a closely similar manner.

The proof for $\Gamma(\mathbf{m}) = A_2$ and even k proceeds by defining the vector $\mathbf{m}$ on vertices of the triangular region of $\mathfrak{a}(H(k+2,k,k,k))$ that is bounded by two mirror lines. For an A_2 vector, all entries on these lines are zero. Free variables α_i and β_i are assigned along the main sub-diagonal, as shown in Figure 5 (continued over the boundary with notional α_0 and β_0, which are $\alpha_0 = \alpha_1$ and $\beta_0 = 0$), and entries for successive sub-diagonals are assigned using the local condition to sweep to the right and down. As B is bipartite, these assignments lead to linear expressions that do not mix α and β

variables for vertices in the main body of the altan. Mixing will occur only on the perimeter. Successive sub-diagonals have patterns (working away from the centre of B):

$$\begin{array}{lccccccccccc}
d=0: & \alpha_0 & & \alpha_1 & & \alpha_2 & & \alpha_3 & & \dots \\
d=1: & & -\alpha_0 & & -\alpha_1 & & -\alpha_2 & & -\alpha_3 & \\
d=2: & & & \alpha_0-\alpha_1 & & \alpha_1-\alpha_2 & & \alpha_2-\alpha_3 & & \dots \\
d=3: & & & & 2\alpha_1-\alpha_0 & & 2\alpha_2-\alpha_1 & & 2\alpha_3-\alpha_2 & \\
d=4: & & & & & \alpha_0-3\alpha_1+\alpha_2 & & \dots & & \dots \\
d=5: & & & & & & -\alpha_0+4\alpha_1-3\alpha_2 & & \dots &
\end{array}$$

leading to general term for sub-diagonal d

$$A_{d,j} = \sum_{i=0}^{\lfloor d/2 \rfloor} (-1)^{d+i} \binom{d-i}{i} \alpha_{i+j}. \tag{8}$$

Similar expressions apply for the entries on the β lattice. For a given k, the pattern is continued until the degree-3 vertices on the altan perimeter are assigned. The boundary condition that all entries on vertices in the vertical mirror line are zero leads to $k/2$ independent equations in β variables. The local condition at the degree-2 vertices of the perimeter leads to a further $k/2$ independent conditions on the α set. Finally, the perimeter pentagonal face at the 'corner' of $\mathfrak{a}(H(k+2,k,k,k))$ disrupts the bipartite pattern; pivoting at vertex p and its neighbours (see Figure 5) leads to two equations linking α and β sets. The conclusion is that all α_i and β_i vanish and $\mathbf{m}$ is the null vector. Similar reasoning is applied for $\Gamma(\mathbf{m}) = A_1$ and odd k.

Hence we have a full symmetry characterisation: $H(k+2,k,k,k)$ has $\eta = 2$, with kernel spanned by a pair of vectors of symmetry E in $\mathbf{D}_3$, and $\mathfrak{a}(H(k+2,k,k,k))$ has $\eta = 3$ with kernel spanned by a triple of vectors with symmetry $A_q + E$ in $\mathbf{D}_3$, where q is 2 for even k and 1 for odd k.

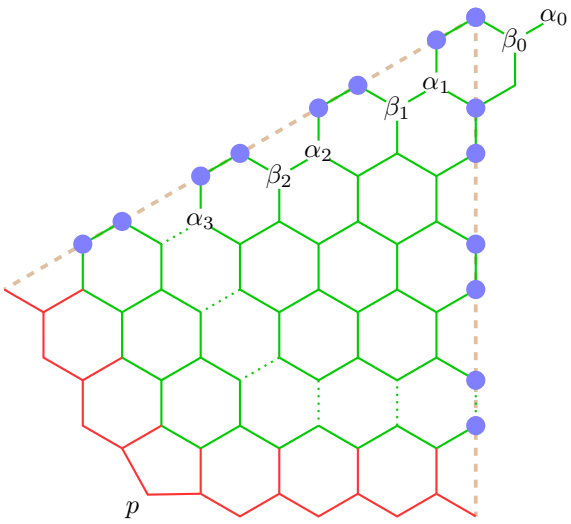

Figure 5: Fundamental region appropriate to an A_2 eigenvector of $\mathfrak{a}(H(k+2,k,k,k))$ with even k, shown explicitly for $k = 6$. Blue filled circles indicate zero entries in the vector that are forced by symmetry. Green edges are present in both parent and altan; red edges are added in the altan. Mirror lines are shown in brown. Notation for variables $\{\alpha_i\}$ and $\{\beta_i\}$ is discussed in the text. Vertex p in the altan breaks the bipartite nature of this region, and allows determination of relationships between $\{\alpha_i\}$ and $\{\beta_i\}$ in the A_2 kernel eigenvector.

3. Concluding remarks

The family of benzenoids characterised here has nullity 2 for the parent and 3 for the first altan, and hence will retain nullity 3 in all subsequent generations of iterated altan [1, Theorem 6]. At each subsequent altanisation, a belt of hexagons will be added, to build up a nanotube structure in which $\mathfrak{a}(H(k+2,k,k,k))$ forms the cap, and steric forces will produce a capped-cylinder morphology. The results discussed in the present paper are pertinent to the theory of magnetic properties of such nanotubes in various charge states, which can also be studied with essentially graph-theoretical methods [29].

Acknowledgement

The work of Nino Bašić is supported in part by the Slovenian Research Agency (Research Programme P1-0294 and Research Projects J1-9187, J1-1691, N1-0140 and J1-2481). Patrick W. Fowler thanks the Leverhulme Trust for an Emeritus Fellowship on the theme of 'Modelling Molecular Currents, Conduction and Aromaticity'.

References

[1] N. Bašić, P. W. Fowler, On the nullity of altans and iterated altans, *MATCH Commun. Math. Comput. Chem.* **88** (2022) 705–745.
[2] N. Bašić, P. W. Fowler, T. Pisanski, Coronoids, patches and generalised altans, *J. Math. Chem.* **54** (2016) 977–1009.
[3] N. Bašić, P. W. Fowler, T. Pisanski, Stratified enumeration of convex benzenoids, *MATCH Commun. Math. Comput. Chem.* **80** (2018) 153–172.
[4] N. Bašić, T. Pisanski, Iterated altans and their properties, *MATCH Commun. Math. Comput. Chem.* **74** (2015) 645–658.
[5] D. M. Bishop, *Group Theory and Chemistry*, Dover Publications, New York, 1993.
[6] G. Brinkmann, G. Caporossi, P. Hansen, A constructive enumeration of fusenes and benzenoids, *J. Algorithms* **45** (2002) 155–166.
[7] C. A. Coulson, H. C. Longuet-Higgins, The electronic structure of conjugated systems I. General theory, *Proc. Roy. Soc. London A* **191** (1947) 39–60.
[8] C. A. Coulson, H. C. Longuet-Higgins, The electronic structure of conjugated systems II. Unsaturated hydrocarbons and their heteroderivatives, *Proc. Roy. Soc. London A* **192** (1947) 16–32.
[9] C. A. Coulson, H. C. Longuet-Higgins, The electronic structure of conjugated systems III. Bond orders in unsaturated molecules, *Proc. Roy. Soc. London A* **193** (1948) 447–456.
[10] C. A. Coulson, H. C. Longuet-Higgins, The electronic structure of conjugated systems IV. Force constants in unsaturated hydrocarbons, *Proc. Roy. Soc. London A* **193** (1948) 457–464.
[11] C. A. Coulson, H. C. Longuet-Higgins, The electronic structure of conjugated systems V. The interaction of two conjugated systems, *Proc. Roy. Soc. London A* **195** (1949) 188–197.
[12] C. A. Coulson, G. S. Rushbrooke, Note on the method of molecular orbitals, *Math. Proc. Camb. Philos. Soc.* **36** (1940) 193–200.
[13] R. Cruz, I. Gutman, J. Rada, Convex hexagonal systems and their topological indices, *MATCH Commun. Math. Comput. Chem.* **68** (2012) 97–108.
[14] J. R. Dias, *Molecular Orbital Calculations Using Chemical Graph Theory*, Springer, Berlin, 1993.
[15] T. K. Dickens, R. B. Mallion, Topological ring currents and bond currents in neutral and dianionic altans and iterated altans of benzene, naphthalene, and azulene, *J. Phys. Chem. A* **125** (2021) 10485–10499.
[16] S. Fajtlowicz, P. E. John, H. Sachs, On maximum matchings and eigenvalues of benzenoid graphs, *Croat. Chem. Acta* **78** (2005) 195–201.
[17] P. W. Fowler, B. T. Pickup, W. Myrvold, T. Z. Todorova, A selection rule for molecular conduction, *J. Chem. Phys.* **131** (2009) 044104.
[18] P. W. Fowler, E. Steiner, Pseudo-π currents: rapid and accurate visualisation of ring currents in conjugated hydrocarbons, *Chem. Phys. Lett.* **364** (2002) 259–266.
[19] I. Gutman, Altan derivatives of a graph, *Iranian J. Math. Chem.* **5** (2014) 85–90.
[20] I. Gutman, Topological properties of altan-benzenoid hydrocarbons, *J. Serbian Chem. Soc.* **79** (2014) 1515–1521.
[21] I. Gutman, B. Borovićanin, Nullity of graphs: an updated survey, *Zb. Rad.* **22** (2011) 137–154.
[22] I. Gutman, S. J. Cyvin, *Introduction to the Theory of Benzenoid Hydrocarbons*, Springer-Verlag, Berlin, 1989.
[23] P. Hansen, C. Lebatteux, M. Zheng, The boundary-edges code for polyhexes, *J. Mol. Struct. THEOCHEM* **363** (1996) 237–247.
[24] E. Hückel, Quantentheoretische Beiträge zum Benzolproblem I. Die Elektronenkonfiguration des Benzols und verwandter Verbindungen, *Z. Phys.* **70** (1931) 204–286.
[25] J. V. Knop, W. R. Müller, K. Syzmanski, N. Trinajstić, *Computer Generation of Certain Classes of Molecules*, SKTH/Kemija u industriji, Zagreb, 1985.
[26] H. C. Longuet-Higgins, Some studies in molecular orbital theory I. Resonance structures and molecular orbitals in unsaturated hydrocarbons, *J. Chem. Phys.* **18** (1950) 265–274.
[27] R. McWeeny, *Coulson's Valence*, Oxford University Press, Oxford, 1979.
[28] G. Monaco, R. Zanasi, Three contra-rotating currents from a rational design of polycyclic aromatic hydrocarbons: altan-corannulene and altan-coronene, *J. Phys. Chem. A* **116** (2012) 9020–9026.
[29] W. Myrvold, P. W. Fowler, J. Clarke, Partitioning Hückel-London currents into cycle contributions, *Chemistry* **3** (2021) 1138–1156.
[30] N. Pavliček, A. Mistry, Z. Majzik, N. Moll, G. Meyer, D. J. Fox, L. Gross, Synthesis and characterization of triangulene, *Nature Nanotech.* **12** (2017) 308–311.
[31] N. Trinajstić, *Chemical Graph Theory, Volume I*, CRC Press, Boca Raton, 1983.
[32] N. Trinajstić, *Chemical Graph Theory, Volume II*, CRC Press, Boca Raton, 1983.
[33] N. Trinajstić, *Chemical Graph Theory*, Mathematical Chemistry Series, Second Edition, CRC Press, Boca Raton, 1992.
[34] N. Trinajstić, S. Nikolić, J. V. Knop, W. R. Müller, K. Syzmanski, *Computational Chemical Graph Theory: Characterization, Enumeration and Generation of Chemical Structures by Computer Methods*, Ellis Horwood, Chichester, 1991.
[35] R. Zanasi, P. Della Porta, G. Monaco, The intriguing class of altan-molecules, *J. Phys. Org. Chem.* **29** (2016) 793–798.
[36] T. Živković, Calculation of the non-bonding molecular orbitals in the Hückel Theory, *Croat. Chem. Acta* **44** (1972) 351–364.